

## Is the Atmospheric Zonal Index Driven by an Eddy Feedback?

STEVEN FELDSTEIN

*Earth System Science Center, The Pennsylvania State University, University Park, Pennsylvania*

SUKYOUNG LEE

*Department of Meteorology, The Pennsylvania State University, University Park, Pennsylvania*

(Manuscript received 2 September 1997, in final form 30 January 1998)

### ABSTRACT

The authors address the question of whether or not eddy feedback plays an important role in driving the anomalous relative angular momentum associated with the zonal index (ZI) in the atmosphere. For this purpose, composites of anomalous relative angular momentum and anomalous eddy angular momentum flux convergence (eddy forcing) are examined with National Centers for Environmental Prediction–National Center for Atmospheric Research Reanalysis data.

By using an empirical orthogonal function analysis, it is found that ZI behavior dominates the summer season of both hemispheres and also the winter season of the Southern Hemisphere. For the summer season, the ZI is characterized by meridional displacements of the midlatitude eddy-driven jet, and for the Southern Hemisphere winter it is characterized by a simultaneous movement of the subtropical and eddy-driven jets in the opposite direction.

For the ZI of each of the above seasons, unfiltered eddy forcing did not exhibit a prominent eddy feedback. However, suggestive evidence for a feedback by high-frequency eddies (period less than 10 days) was found. These eddies act to prolong the lifetime of the ZI anomalies against the dissipative influences of both low-frequency (period greater than 10 days) and cross-frequency (eddy fluxes that involves the product of high- and low-frequency disturbances) eddy forcing and the friction torque.

### 1. Introduction

Within the past several years, there has been a controversy as to the manner in which the eddies force meridional displacements of the zonally averaged zonal jet. These meridional jet displacements, known as the zonal index (ZI), have been found in observations (Rogers and van Loon 1982; Kidson 1985, 1986, 1988; Nigam 1990; Karoly 1990; Lyons and Hundermark 1992; Hartmann 1995; Hartmann and Lo 1998) and in idealized numerical models (Robinson 1991, 1996; Yu and Hartmann 1993; Lee and Feldstein 1996; Feldstein and Lee 1996). The modeling studies of Robinson (1991) and Yu and Hartmann (1993) present results suggesting that the ZI anomaly is maintained by an eddy feedback in the sense that eddies are altered by the zonal mean anomaly in such a manner so as to reinforce the zonal mean anomaly. In contrast, the modeling studies of Lee and Feldstein (1996) and Feldstein and Lee (1996) suggest that an eddy feedback is not an important part of

the flow evolution for the ZI. Their evidence for a lack of an eddy feedback was the fact that the eddy forcing of the ZI anomaly was confined to a period of time when the ZI anomaly was growing. After the ZI anomaly attained its maximum amplitude, the eddy forcing rapidly declined and lacked coherent spatial structure. In another modeling study, Robinson (1996) found evidence of an eddy feedback that depended upon the strength of the surface friction, with an eddy feedback being prominent (absent) if the surface friction is sufficiently strong (weak).

The essence of wave–zonal mean flow interaction associated with ZI behavior can be simply described by the equation for the tendency of the vertically integrated zonal mean zonal wind in a quasigeostrophic system, that is,

$$\partial\{\bar{u}\}/\partial t = -\partial\{\overline{u'v'}\}/\partial y - D, \quad (1)$$

where  $u$  and  $v$  are the zonal and meridional winds, respectively, with an overbar denoting a zonal average, prime showing a deviation from a zonal average, curly brackets indicating a vertical integral, and  $D$  is the surface drag. This indicates that only the vertically integrated eddy momentum flux convergence and the surface drag can alter the vertically integrated zonal mean zonal wind.

---

*Corresponding author address:* Dr. Steven Feldstein, Earth System Science Center, The Pennsylvania State University, 248 Deike Building, University Park, PA 16802.  
E-mail: sbf@essc.psu.edu

When addressing the existence of an eddy feedback, it is important to note that examining terms in (1) averaged over a sufficiently long time period and/or at the time of the maximum zonal mean zonal wind anomaly can lead to a misleading conclusion; for a sufficiently long time average,  $\partial\{\bar{u}\}/\partial t \approx 0$ , and at the time of the maximum zonal mean zonal wind anomaly,  $\partial\{\bar{u}\}/\partial t$  is again equal to zero. Such a zero  $\partial\{\bar{u}\}/\partial t$  requires that the vertically integrated eddy momentum flux convergence *must* balance the surface drag, whether or not an eddy feedback is operating. Nevertheless, the occurrence of this balance might lead one to conclude that the ZI anomaly is maintained by an eddy feedback against the effect of surface friction.

Given the above pitfall, in this study, we address the relevance of eddy feedback processes for the ZI in the atmosphere, by examining the full composite temporal evolution of both the zonal mean vertically integrated relative angular momentum and eddy angular momentum flux convergence. However, it is important to emphasize that although a composite analysis can demonstrate that an eddy feedback is not taking place, the converse is not the case, as this procedure cannot definitively show that an eddy feedback is indeed occurring. To demonstrate an eddy feedback, it would be necessary to show that there is a mutual reinforcement taking place between the zonal mean flow and the eddies, which is beyond the scope of this study. Nevertheless, if an eddy feedback is indeed relevant, the composite analysis will yield results consistent with such a process, allowing one to make a suggestive statement on the role of an eddy feedback.

The data and methodology used in this study are presented in section 2, followed by the results in section 3, and the concluding remarks in section 4.

## 2. Data and methodology

This study uses daily (0000 UTC) National Centers for Environmental Prediction–National Center for Atmospheric Research (NCEP–NCAR) Reanalysis data, which extends from 1 January 1979 to 31 December 1995. All fields are truncated at a horizontal resolution of rhomboidal 30. Two primary quantities will be evaluated in this study: the vertically integrated relative angular momentum, denoted by  $M_R$ , and the vertically integrated eddy angular momentum flux convergence, hereafter referred to as the eddy forcing. These quantities are conveniently related in sigma coordinates through the equation

$$\frac{\partial M_R}{\partial t} = -\frac{1}{\cos\theta} \int_0^{2\pi} \int_0^1 \frac{\partial}{\partial\theta} \left( \frac{up_s v \cos^2\theta}{g} \right) a \cos\theta \, d\sigma \, d\lambda + T_F + T_M + T_C + T_G, \quad (2)$$

where

$$M_R(\theta, t) = \frac{a^2}{g} \int_0^{2\pi} \int_0^1 p_s u \cos^2\theta \, d\sigma \, d\lambda; \quad (3)$$

$p_s$  denotes the surface pressure;  $\sigma$ ,  $\lambda$ , and  $\theta$  are the vertical, longitudinal, and latitudinal coordinates, respectively;  $t$  is time;  $a$  is the earth's radius; and  $g$  is the gravitational acceleration. The various torques are  $T_F$ , the friction torque;  $T_M$ , the mountain torque;  $T_C$ , the Coriolis torque (see Weickmann and Sardeshmukh 1994); and  $T_G$ , the gravity wave drag torque. For times of large ZI, we find that the dominant terms on the rhs of (2) are the eddy angular momentum flux convergence, that is, the  $u'(p_s v)'$  contribution to the integrand of the first term on the rhs of (2), that is, the eddy forcing, and the friction torque  $T_F$ . The remaining terms on the rhs of (2) are typically about 3–4 times smaller in magnitude than the maximum eddy angular momentum flux convergence or  $T_F$ .

The vertical integrals that are used to calculate the  $M_R$  and eddy forcing extend over all 28 of the reanalysis model's sigma levels, that is, from  $\sigma = 0.995$  to  $\sigma = 0.0027$ . Essentially identical results to those presented in section 3 are obtained if this vertical integration is restricted to the troposphere. Nevertheless, complete vertical integrals are retained in order to obtain the best possible balance in (2). The  $M_R$  and eddy forcing are also presented as integrals over equally spaced latitudinal bands of  $2.25^\circ$ .

The analysis will be performed for two separate time periods, November through March and May through September, for both hemispheres. These periods will be referred to as the Northern Hemisphere (NH) winter and Southern Hemisphere (SH) summer, and the NH summer and SH winter, respectively. In this study, both unfiltered and filtered eddy forcing will be presented. For the filtered fluxes, both  $u'$  and  $(p_s v)'$  are separated into high-frequency (hereafter HF) eddy (period less than 10 days), low-frequency (hereafter LF) eddy (period greater than 10 days with the seasonal mean subtracted), and stationary eddy components. This filtering is performed with a 31-point digital filter. This decomposition allows the filtered eddy angular momentum fluxes to be written as

$$\begin{aligned} \overline{u'(p_s v)'} &= \overline{u'_M(p_s v)'_M} + \overline{u'_M(p_s v)'_L} + \overline{u'_M(p_s v)'_H} \\ &+ \overline{u'_L(p_s v)'_M} + \overline{u'_H(p_s v)'_M} + \overline{u'_H(p_s v)'_H} \\ &+ \overline{u'_H(p_s v)'_L} + \overline{u'_L(p_s v)'_H} + \overline{u'_L(p_s v)'_L}, \end{aligned} \quad (4)$$

where the subscripts  $H$ ,  $L$ , and  $M$  denote high-frequency, low-frequency, and stationary eddies, respectively.

Anomalies of  $M_R$  and the eddy forcing are defined relative to the seasonal cycle. For both quantities, the seasonal cycle is estimated by first calculating the climatological value for each calendar day, followed by a smoothing with a 20-day low-pass digital filter. The results to be shown in this study were found to be insensitive to the cutoff frequency of this filter.

The definition of the ZI is based on both the spatial

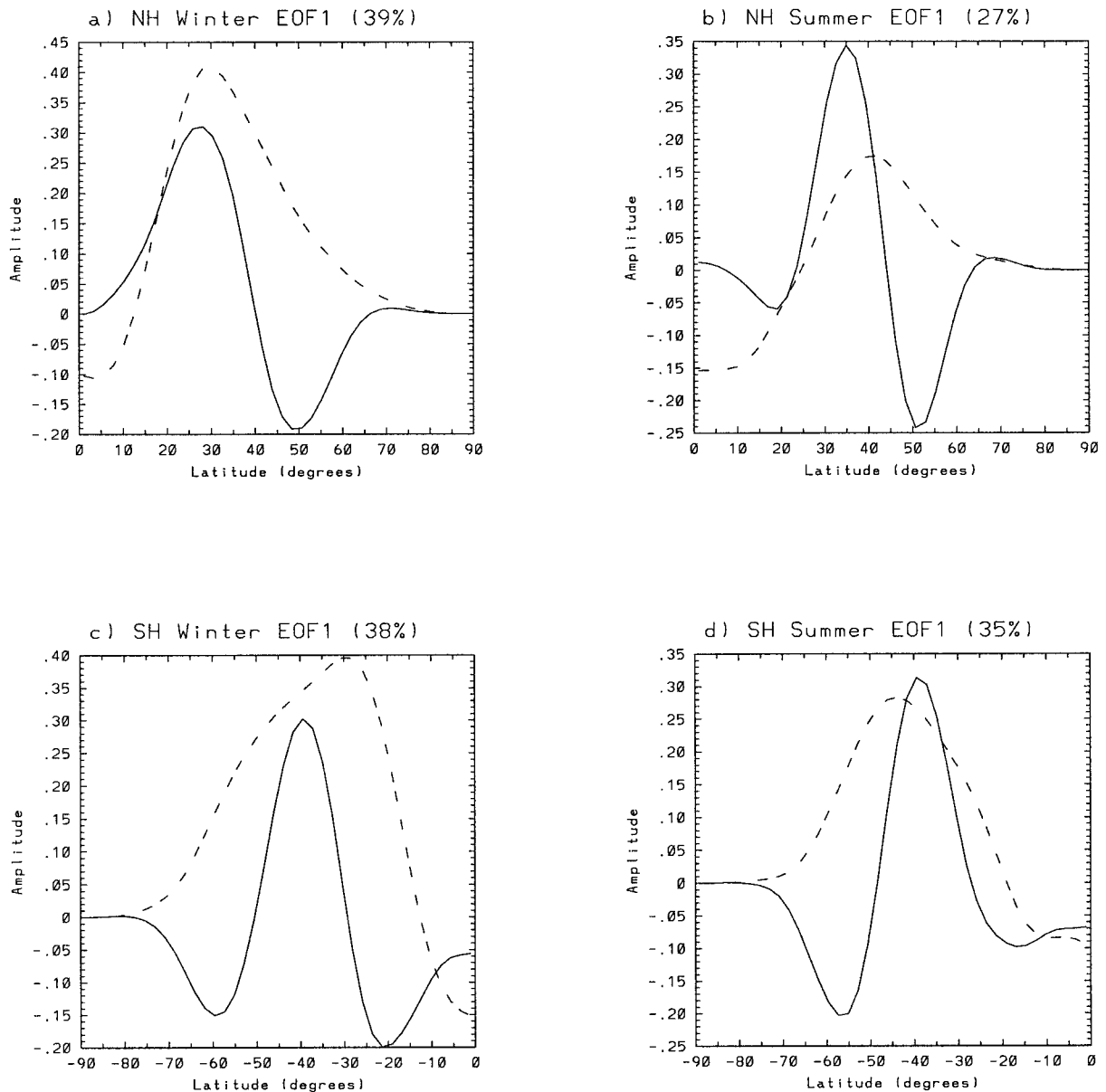


FIG. 1. EOF1 (solid line) and seasonal mean relative angular momentum (dashed line) for (a) the NH winter, (b) the NH summer, (c) the SH winter, and (d) SH summer.

structure of an empirical orthogonal function (EOF) of the hemispheric  $M_R$  and the sign of its principal component (expansion coefficient). If an EOF exhibits a dipolar spatial structure with its node located near the latitude of the jet maximum, then that EOF represents latitudinal jet displacements. For such an EOF, the sign of the principal component that corresponds to poleward (equatorward) jet displacements is referred to as the high (low) ZI. Also, the phase of an EOF is defined by the sign of its principal component. We define the occurrence of a persistent episode based on the requirement that the pattern correlation, defined as the spatial cross-correlation between the anomalous  $M_R(\theta,$

$t)$  and the anomalous  $M_R(\theta, t + \tau)$ , where  $\tau$  is a time lag, exceed the 95% confidence level for 5 or more consecutive days (see Feldstein and Lee 1996 for details). The onset day is defined as the first day of a persistent episode. Another requirement placed on the onset day is that the magnitude of the principal component of the EOF of interest exceeds one standard deviation, otherwise that persistent episode is excluded. Furthermore, when the onset day of one persistent episode occurs within 15 days of the last day of the previous persistent episode, the latter episode is discarded and is regarded as being part of the earlier episode. The main results of this study will be presented

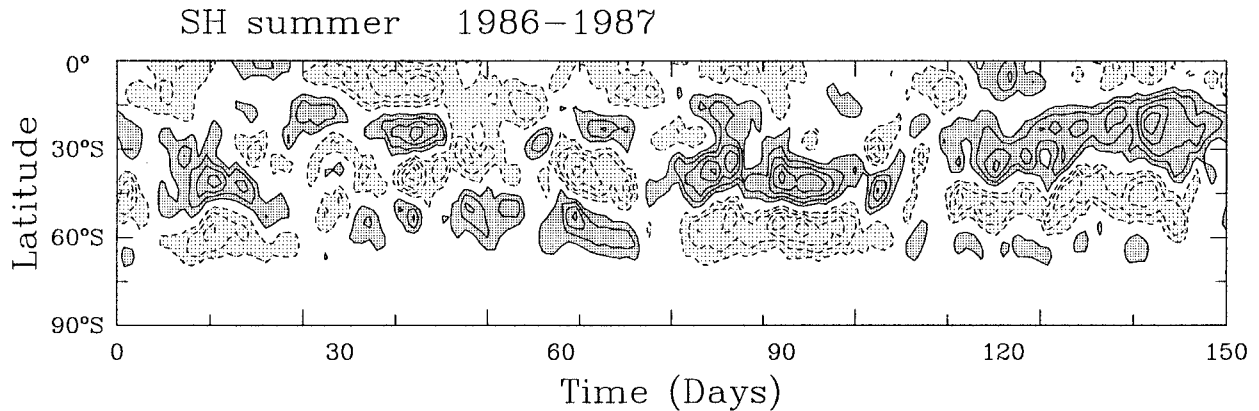


FIG. 2. Latitude–time diagram of anomalous  $M_R/1.0 \times 10^{24}$  for the SH summer of 1986–87. The contour interval is  $0.4 \text{ kg m}^{-2} \text{ s}^{-1}$ . Solid contours are positive, dashed contours negative, and the zero contour is omitted. Shaded values exceed a magnitude of  $0.4 \text{ kg m}^{-2} \text{ s}^{-1}$ , with dark (light) shading denoting positive (negative) values.

as composites of anomalous eddy forcing and  $M_R$  relative to the onset day.

### 3. Results

The various EOF1s (the first EOF) of the anomalous  $M_R$ , for both seasons and hemispheres, are shown in Fig. 1. Each EOF1 was found to be distinct (North et al. 1982). Other observational studies, for example, Karoly (1990), Nigam (1990), Lyons and Hundermark (1992), and Hartmann and Lo (1998), find extremely similar spatial structures for the EOF1. Superimposed upon the EOF1s are the climatological  $M_R$  fields for the same season. The role of each EOF1 can be inferred by first comparing the location of the maximum climatological  $M_R$  with that of the observed upper-tropospheric zonal mean jet maxima (cf. Peixoto and Oort 1992, 154). For the NH and SH winters, the climatological  $M_R$  maxima coincide with the subtropical jet maxima, and for the NH and SH summers, the climatological  $M_R$  maximum occur very close to the eddy-driven, or polar front, jet maxima. Also, for the SH winter, there is a poorly defined eddy-driven jet between  $50^\circ$  and  $55^\circ\text{S}$  (Peixoto and Oort 1992).

The above relationships imply the following interpretation for the EOF1; the NH winter EOF1 primarily represents a strengthening and weakening of the subtropical jet, the NH and SH summer EOF1s correspond to a latitudinal movement of the eddy-driven jet, and the SH winter EOF1 represents simultaneous movements of both the subtropical and eddy-driven jets in the opposite direction. Although not shown, composites of  $M_R$  for large values of the principal component of SH winter EOF1 indicate that this EOF corresponds to a coalescence and spreading apart of the two jets. Thus, ZI behavior is indeed the dominant form of variability for the SH summer, SH winter, and NH summer. For the NH and SH summers, this behavior corresponds to

an eddy-driven jet ZI, and for the SH winter it corresponds to a mix of an eddy-driven and subtropical jet ZI.

An example showing several persistent ZI events during one particular season (1986–87 SH summer) is presented in Fig. 2. These persistent ZI events can be identified by  $M_R$  anomalies that have a spatial structure that closely resembles the SH summer EOF1, for example, the low index event beginning on day 80. It is important to note that the technique used in this study selects for persistent events with little latitudinal propagation. As can be seen in Fig. 2, such events do indeed occur, although  $M_R$  anomalies in both hemispheres and seasons typically exhibit poleward propagation, as found by Feldstein (1998).

We next examine composites of anomalous  $M_R$  at different lags relative to the onset day (lag 0) for each hemisphere and season (see Fig. 3). The number of persistent events that make up these composites are summarized in Table 1. In Fig. 3, the contours illustrate the anomalous composite  $M_R$  and the shading corresponds to those values that are statistically significant above the 95% confidence level for a two-sided  $t$  test. This test of statistical significance is determined relative to a zero mean, since the seasonal cycle has been removed at each latitude. If we define the length of a persistent episode as corresponding to the amount of time for which the anomalous  $M_R$  is statistically significant above the 95% confidence level, then it can be seen that most persistent episodes last between 10 and 20 days. In each frame in Fig. 3, it can be seen that the  $M_R$  anomalies grow more rapidly than they decay. However, it is important to note that this temporal asymmetry is due to the compositing procedure (see Feldstein and Lee 1996 for additional details), which selectively favors rapidly growing  $M_R$  anomalies for the onset day. Nevertheless, we concentrate on composites based on the onset

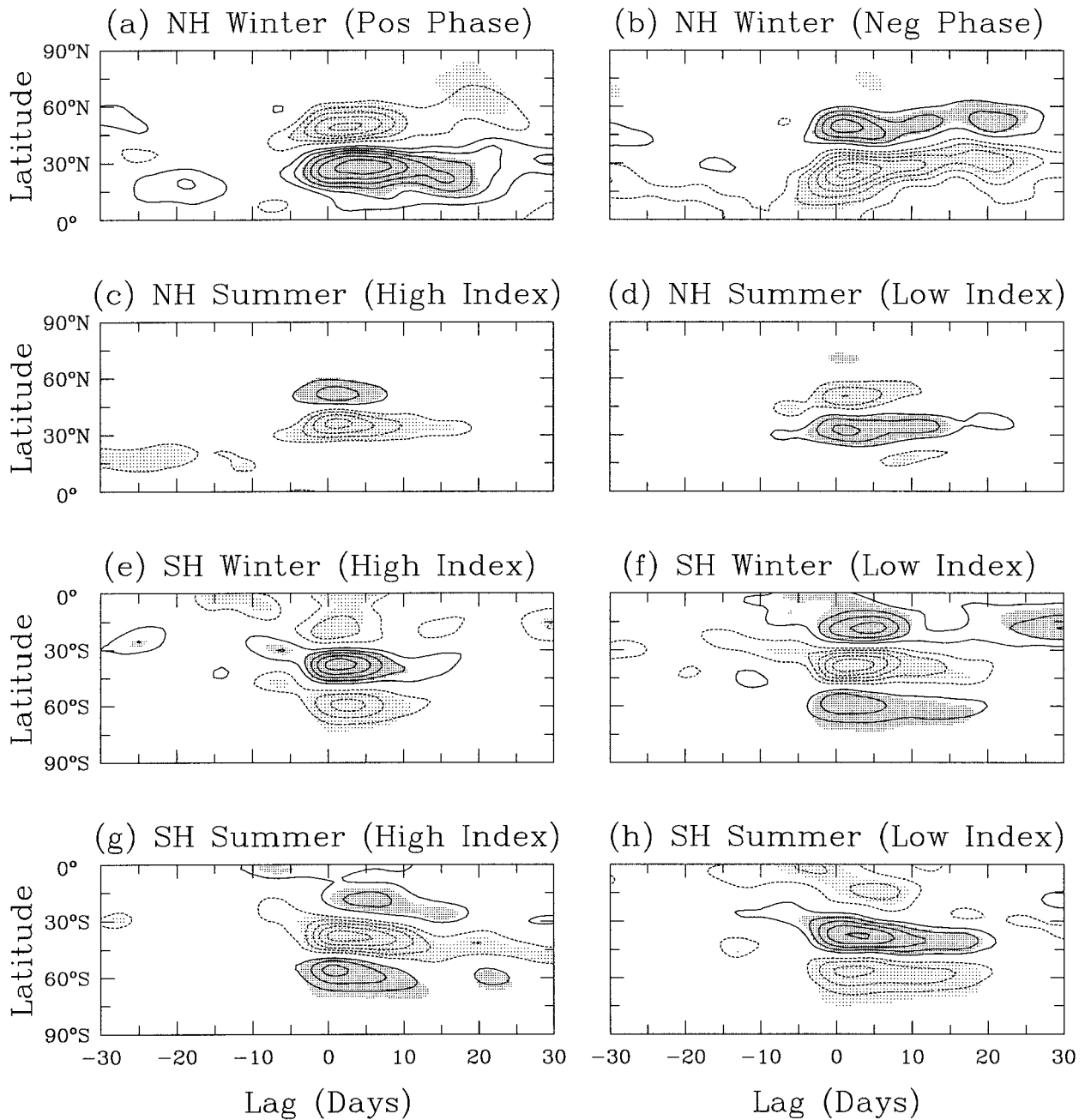


FIG. 3. Anomalous composite  $M_g/1.0 \times 10^{24}$  as a function of lag and latitude for (a) NH winter, positive phase; (b) NH winter, negative phase; (c) NH summer, high index; (d) NH summer, low index; (e) SH winter, high index; (f) SH winter, low index; (g) SH summer, high index; and (h) SH summer, low index. The contour interval is  $0.2 \text{ kg m}^2 \text{ s}^{-1}$ . Lag zero corresponds to the onset day. Solid contours are positive, dashed contours negative, and the zero contour is omitted. Shaded values exceed the 95% confidence level, with dark (light) shading denoting positive (negative)  $t$  values.

TABLE 1. The number of persistent events.

NH winter	Positive phase	19	Negative phase	34
NH summer	High index	27	Low index	25
SH winter	High index	27	Low index	28
SH summer	High index	34	Low index	28

day, because the amplitude of the eddy forcing is largest at this time.

#### a. Unfiltered eddy forcing

For each season, the anomalous unfiltered eddy forcing (see Fig. 4) is essentially confined to the time period

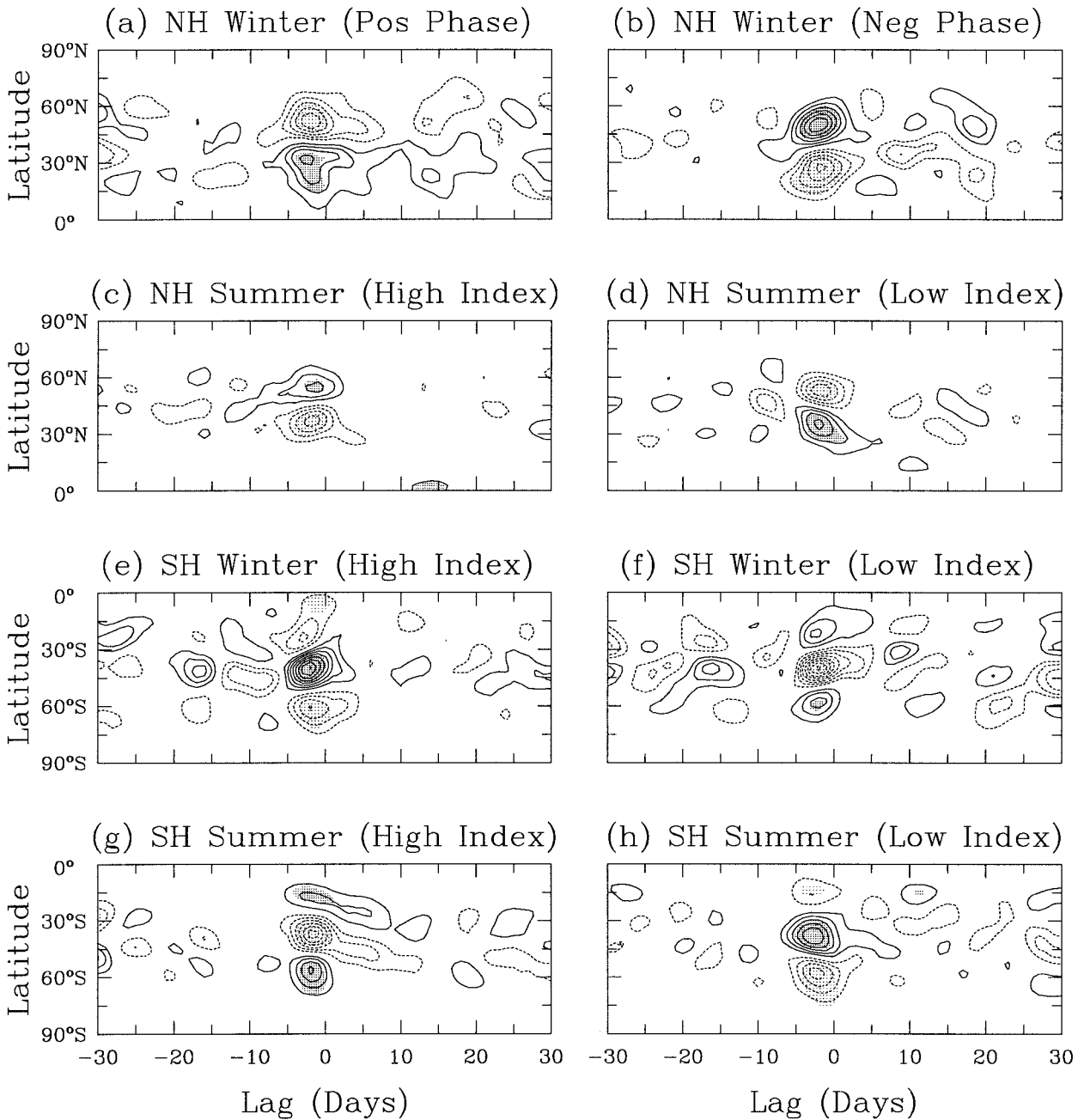


FIG. 4. Anomalous eddy angular momentum flux convergence as a function of lag and latitude for (a) NH winter, positive phase; (b) NH winter, negative phase; (c) NH summer, high index; (d) NH summer, low index; (e) SH winter, high index; (f) SH winter, low index; (g) SH summer, high index; and (h) SH summer, low index. These quantities are divided by  $1.0 \times 10^{18}$ . Lag zero corresponds to the onset day. The contour interval in (a) and (b) is  $0.6 \text{ kg m}^2 \text{ s}^{-2}$  and in (c)–(h) is  $0.4 \text{ kg m}^2 \text{ s}^{-2}$ . Solid contours are positive, dashed contours negative, and the zero contour is omitted. Shaded values exceed the 95% confidence level, with dark (light) shading denoting positive (negative)  $t$  values.

when the  $M_R$  anomalies are growing (see Fig. 3). Once the  $M_R$  anomalies attain their maximum amplitude, the amplitude of the eddy forcing is substantially reduced (the anomalous eddy forcing is no longer statistically significant at this time) and, shortly thereafter, the anom-

alous eddy forcing remains disorganized with much smaller amplitude.

Returning to the question raised in the introduction, are the  $M_R$  anomalies maintained by an eddy feedback? Comparison between Figs. 3 and 4 leads us to conclude

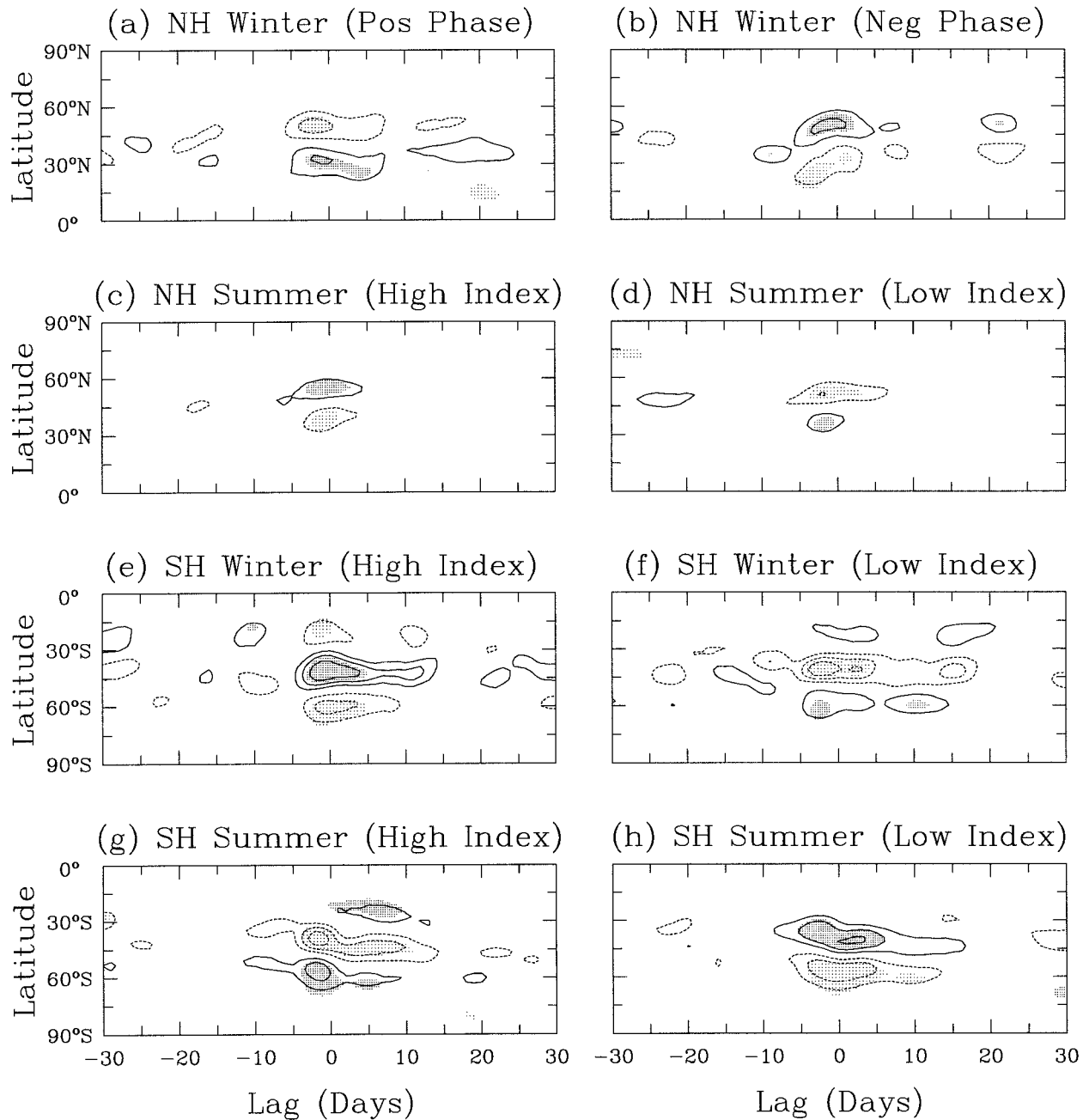


FIG. 5. Same as Fig. 4 except for the anomalous HF eddy angular momentum flux convergence.

that with the exception of the positive phase of the NH winter (recall that EOF1 for the NH winter does not correspond to the ZI), there is essentially no feedback by the unfiltered transient eddies. This is simply because, after the  $M_R$  anomalies reach their maximum amplitude, the anomalous eddy forcing is weak, mostly disorganized, and no longer projects onto the  $M_R$  anomalies. As a result, the decay of the  $M_R$  anomalies due to the friction torque is little influenced by the eddy

forcing. (The anomalous friction torque, although not shown, is found to have essentially the same spatial and temporal structure as the anomalous  $M_R$  in Fig. 3, but with opposite sign. Thus, the anomalous friction torques also persist between 10 and 20 days.) The high index of the SH summer may appear to be an exception. However, a close inspection reveals that by several days after the maximum anomalous  $M_R$ , the anomalous eddy forcing and  $M_R$  are in spatial quadrature.

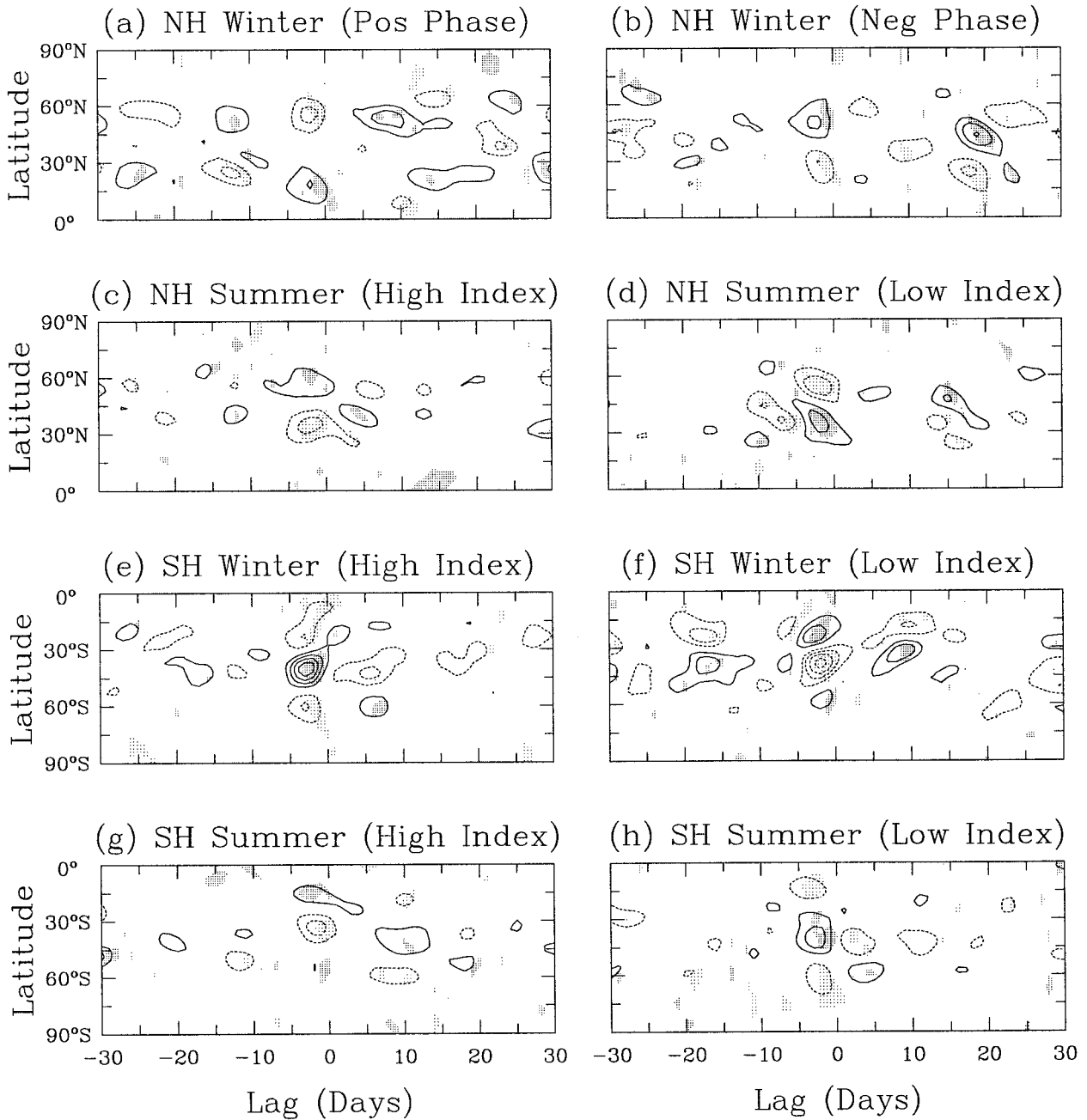


FIG. 6. Same as Fig. 4 except for the anomalous summation of the LF and CF eddy angular momentum flux convergence.

The above results also point to the fact that to evaluate the occurrence of an eddy feedback, it is necessary to examine the full temporal evolution of the anomalous  $M_R$  and eddy forcing fields. As discussed in the introduction, the examination of the eddy forcing composites solely at times of extrema in the anomalous  $M_R$  might lead one to the incorrect interpretation that an eddy feedback is occurring. However, as can be seen in Figs. 3 and 4, the eddy forcing at the time of maximum anomalous  $M_R$  is just a small remnant

of its value from several days earlier, consistent with the idea that an eddy feedback is most likely not taking place.

#### b. Filtered eddy forcing

A different perspective can be obtained by examining the anomalous HF eddy forcing,  $\overline{u'_H(p_s v)_H}$  [see (4)]. This quantity is illustrated for each season in Fig. 5. The most striking feature of the anomalous

HF eddy forcing is that it persists for a markedly longer period of time than does the anomalous unfiltered eddy forcing. In fact, in some cases, the anomalous HF eddy forcing extends throughout most of the persistent episode. The prolonged nature of the HF eddy forcing, well beyond the lifetime of a single synoptic-scale disturbance, suggests that an eddy feedback may indeed be taking place for disturbances within this frequency band, even though there is no apparent feedback within the unfiltered eddy field. However, as stated in the introduction, the above analysis cannot demonstrate with certainty that an eddy feedback is indeed occurring. For example, the composite analysis does not rule out the possibility that the lengthy period of organized anomalous HF eddy forcing simply results from the low-frequency variation of HF transients. One plausible example is a baroclinic wave packet (Lee and Held 1993).

The sum of the anomalous low-frequency and cross-frequency (hereafter CF, which involves products between high- and low-frequency eddies) eddy forcing is shown in Fig. 6. With the exception of the NH winter, where the stationary eddies are found to make an important contribution to the eddy forcing [the second through fifth terms in (4)], it can be seen that the sum of the anomalous LF and CF eddy forcing terms enhances the growth (decay) of the  $M_R$  anomalies before (after) the  $M_R$  anomaly maxima. A separate examination of the anomalous LF and CF eddy forcing finds that these terms have a similar spatial structure and amplitude, indicating that they play similar roles in the evolution of the  $M_R$  anomalies.

The overall picture from the above results is consistent with an eddy feedback by the HF transients, and these eddies, typically associated with synoptic-scale disturbances (Hoskins et al. 1983), prolong the lifetime of the  $M_R$  anomalies against the effects of both the friction torque and the LF and CF eddy fluxes. Returning to the ZI modeling studies that suggest that ZI anomalies are maintained by an eddy feedback, Robinson (1991) and Yu and Hartmann (1993) find that the eddy forcing is dominated by the HF eddies and that eddy forcing from other frequency bands is much smaller. Presumably it is the weak influence of the LF and CF transients in Robinson (1991) and Yu and Hartmann (1993) that accounts for the prolonged unfiltered eddy forcing of the ZI in their models.

As discussed above, the positive phase of the NH winter exhibits characteristics different from those for the other seasons. This is found to be due to the terms in (4) that involve the product of low-frequency and stationary eddy terms, which prolong the persistence of the anomaly. It is this characteristic that most likely accounts for the fact that the NH winter EOF1 is different from that of the "classic" ZI, as described in the beginning of this section.

#### 4. Concluding remarks

The aim of this study was to examine the possible role of an eddy feedback in the prolongation of the anomalous  $M_R$  field associated with the ZI. For both the high and low ZI, during the SH winter and summer and the NH summer (the ZI was not the dominant form of variability for the NH winter), no prominent eddy feedback was found if the eddy fields remained unfiltered. However, when the eddy field was divided into different frequency bands, evidence was provided that is consistent with an eddy feedback by the anomalous HF transient eddies. Such behavior suggests that a HF transient eddy feedback may indeed prolong the  $M_R$  anomaly against the dissipative effects of both the friction torque and the CF and LF eddy fluxes.

Several important questions are raised by the results of this study: 1) Why do the LF and CF eddy fluxes contribute substantially to both the growth and the decay of the  $M_R$  anomalies? and 2) what type of eddy structures can be identified with the LF and CF transients? The answers to these questions must await further research involving a detailed analysis of the horizontal structure of the low-frequency transient eddies at all stages during the  $M_R$  anomaly evolution.

*Acknowledgments.* This research was supported by the National Science Foundation through Grants ATM-9416701 and ATM-9712834. We also thank the NOAA Climate Diagnostics Center for providing us with the NCEP-NCAR reanalysis dataset.

#### REFERENCES

- Feldstein, S. B., 1998: An observational study of the intraseasonal poleward propagation of zonal mean flow anomalies. *J. Atmos. Sci.*, **55**, 2516–2529.
- , and S. Lee, 1996: Mechanisms of zonal index variability in an aquaplanet GCM. *J. Atmos. Sci.*, **52**, 3541–3555.
- Hartmann, D. L., 1995: A PV view of zonal flow vacillation. *J. Atmos. Sci.*, **52**, 2561–2576.
- , and F. Lo, 1998: Wave-driven zonal flow vacillation in the Southern Hemisphere. *J. Atmos. Sci.*, **55**, 1303–1315.
- Hoskins, B. J., I. N. James, and G. H. White, 1983: The shape, propagation and mean-flow interaction of large-scale weather systems. *J. Atmos. Sci.*, **40**, 1595–1612.
- Karoly, D. J., 1990: The role of transient eddies in low-frequency zonal variations of the Southern Hemisphere. *Tellus*, **42A**, 41–50.
- Kidson, J. W., 1985: Index cycles in the Northern Hemisphere during the Global Weather Experiment. *Mon. Wea. Rev.*, **113**, 607–623.
- , 1986: Index cycles in the Southern Hemisphere during the Global Weather Experiment. *Mon. Wea. Rev.*, **114**, 1654–1663.
- , 1988: Indices of the Southern Hemisphere zonal wind. *J. Climate*, **1**, 183–194.
- Lee, S., and I. M. Held, 1993: Baroclinic wave packets in models and observations. *J. Atmos. Sci.*, **50**, 1413–1428.
- , and S. B. Feldstein, 1996: Mechanisms of zonal index evolution in a two-layer model. *J. Atmos. Sci.*, **53**, 2232–2246.
- Lyons, S. W., and B. Hundermark, 1992: Zonal-wind oscillations

- over the Western Hemisphere during winter: Further evidence of a zonal-eddy relationship. *Mon. Wea. Rev.*, **120**, 1878–1899.
- Nigam, S., 1990: On the structure of variability of the observed tropospheric and stratospheric zonal-mean zonal wind. *J. Atmos. Sci.*, **47**, 1799–1813.
- North, G. R., T. L. Bell, R. F. Cahalan, and F. J. Moeng, 1982: Sampling errors in the estimation of empirical orthogonal functions. *Mon. Wea. Rev.*, **110**, 699–706.
- Peixoto, J. P., and A. H. Oort, 1992: *Physics of Climate*. American Institute of Physics, 520 pp.
- Robinson, W., 1991: The dynamics of the zonal index in a simple model of the atmosphere. *Tellus*, **43A**, 295–305.
- , 1996: Does eddy feedback sustain variability in the zonal index? *J. Atmos. Sci.*, **53**, 3556–3569.
- Rogers, J. C., and H. van Loon, 1982: Spatial variability of sea level pressure and 500 mb height anomalies over the Southern Hemisphere. *Mon. Wea. Rev.*, **110**, 1375–1392.
- Weickmann, K. M., and P. D. Sardeshmukh, 1994: The atmospheric angular momentum cycle associated with a Madden–Julian oscillation. *J. Atmos. Sci.*, **51**, 3194–3208.
- Yu, J. Y., and D. L. Hartmann, 1993: Zonal flow vacillation and eddy forcing in a simple GCM of the atmosphere. *J. Atmos. Sci.*, **50**, 3244–3259.

